Environmental Science & Technology

Article

pubs.acs.org/est

Bacterial Inactivation by a Singlet Oxygen Bubbler: Identifying Factors Controlling the Toxicity of $^1O_2$ Bubbles

Dorota Bartusik,[†] David Aebisher,[†] Alan M. Lyons,[‡] and Alexander Greer*[,†]

[†]Department of Chemistry, Brooklyn College, City University of New York, Brooklyn, New York 11210, United States

[‡]Department of Chemistry, College of Staten Island, City University of New York, Staten Island, New York 10314, United States

ABSTRACT: A microphotoreactor device was developed to generate bubbles (1.4 mm diameter, 90 μL) containing singlet oxygen at levels toxic to bacteria and fungus. As singlet oxygen decays rapidly to triplet oxygen, the bubbles leave behind no waste or byproducts other than O_2. From a comparative study in deaerated, air saturated, and oxygenated solutions, it was reasoned that the singlet oxygen bubbles inactivate *Escherichia coli* and *Aspergillus fumigatus*, mainly by an oxygen gradient inside and outside of the bubble such that singlet oxygen is solvated and diffuses through the aqueous solution until it reacts with the target organism. Thus, singlet oxygen bubble toxicity was inversely proportional to the amount of dissolved oxygen in solution. In a second mechanism, singlet oxygen interacts directly with *E. coli* that accumulate at the gas–liquid interface although this mechanism operates at a rate approximately 10 times slower. Due to encapsulation in the gaseous core of the bubble and a 0.98 ms lifetime, the bubbles can traverse relatively long 0.39 mm distances carrying $^1O_2$ far into the solution; by comparison the diffusion distance of $^1O_2$ fully solvated in H_2O is much shorter (~150 nm). Bubbles that reached the outer air–water interface contained no $^1O_2$. The mechanism by which $^1O_2$ deactivated organisms was explored through the addition of detergent molecules and Ca^{2+} ions. Results indicate that the preferential accumulation of *E. coli* at the air–water interface of the bubble leads to enhanced toxicity of bubbles containing $^1O_2$. The singlet oxygen device offers intriguing possibilities for creating new types of disinfection strategies based on photodynamic ($^1O_2$) bubble carriers.

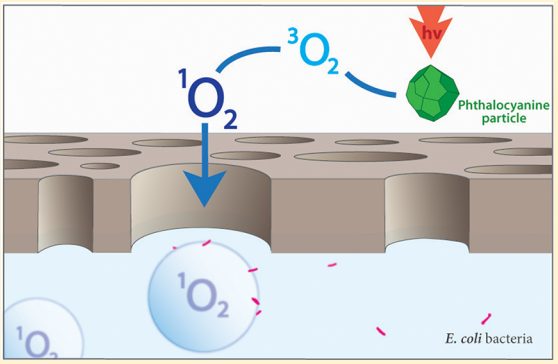

INTRODUCTION

Visible-light photocatalysis holds promise for the treatment of microbe-tainted water,[1−4] although factors such as water turbidity and photosensitizer breakdown can be problems.[5,6] Rather than using a photocatalyst in water, a significant advance could emerge from a unique sensitized disinfection method, which carries singlet oxygen ($^1O_2$) in bubbles. Singlet oxygen bubble technology is available only recently,[7] and foundations for understanding $^1O_2$ reactions at the gas bubble–water interface need to be further develped.[8] Singlet oxygen bubbles may be particularly useful in water disinfection, as $^1O_2$ bubbles leave behind no waste or byproducts.

Unlike photocatalytic/heterogeneous disinfection methods,[9−12] $^1O_2$ bubble disinfection techniques have never been described. Here, we report a comparative study on singlet oxygen bubble inactivation of *Escherichia coli* and *Aspergillus fumigatus* in deaerated and aerobic solutions as a function of a detergent and Ca^{2+} ions. For this study, we used a portable $^1O_2$ photoreactor that has recently been reported[7] (cross-sectional schematic image of the device is shown in Figure 1). The device was loaded with phthalocyanine sensitizer particles and was coupled to a diode laser via an optical fiber and to an O_2 gas tank via a feed tube. Oxygen gas flows over the sensitizer particles while the particles, kept dry by a polyethethylene membrane, are illuminated with 669 nm laser light.

The results point to a mechanism dominated by mass transfer where molecular $^1O_2$ diffuses across the gas–liquid bubble interface into a fully solvated state in solution. A secondary mechanism occurs when singlet oxygen in the gas phase collides and reacts with microbes that accumulate at the gas–liquid interface without diffusion. The latter mechanism is independent of dissolved oxygen concentration and is much slower than the dissolution mechanism.

EXPERIMENTAL SECTION

Reagents and Instrumentation. The chemicals and reagents used were of reagent grade and were not purified before use. Deionized water was purified using a U.S. Filter Corporation deionization system (Vineland, NJ). The membrane contained interpenetrating pores and was manufactured from ultrahigh molecular weight polyethylene with a nominal pore area of 85% for each membrane (Millipore SureVent UPE Membranes, Billerica, MA).

The photosensitizer was a Si phthalocyanine, axially functionalized as the *bis*-amino phthalocyanine derivative **1**,

Received: September 12, 2012
Revised: October 14, 2012
Accepted: October 18, 2012
Published: October 18, 2012

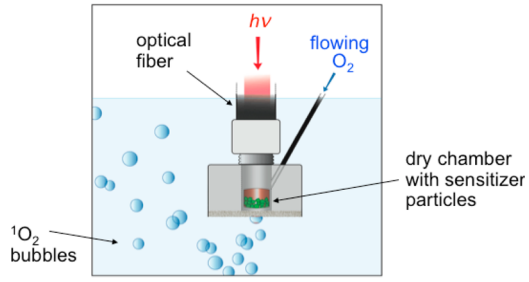

Figure 1. Cross-section illustration of the $^1O_2$ bubble generation system,[7] which was operated in a horizontal or tilted position, consisting of a chamber (5.7 mm diameter, 5.3 mm height) loaded with silicon phthalocyanine glass sensitizer particles (average diameter 150 μm), a hydrophobic microporous membrane (0.05 μm pores and a capillary pressure sufficiently high to exclude water), an O_2 gas feed tube, a 669-nm diode laser coupled to a fiber optic where the light entered the top portion of the device at the SMA coupler. The sensitizer particles are shown as a cutaway view of the device chamber. When immersed in water, the device bubbles $^1O_2$, but the sensitizer remains shielded from water. The bubbles penetrate 7 mm into the solution and then reach the outer solution−air interface.

which reacted with 3-glycidyloxypropyl-trimethoxysilane (GPTMS) forming a glass via a sol−gel process as described previously (Figure 2).[7] The glass sensitizer was ground to 150 μm-sized particles. The device was filled with 35 mg of the sensitizer particles (total number of particles 14 700). The surface area of each sensitizer particle was ∼0.070 mm^2. None of the sensitizer particles escaped the device and entered the water phase. The sensitizer contained a strong absorption in the 670 region to match the 669 nm output of the diode laser.

Diode and Nd:YAG lasers were used as described previously.[7] Briefly, optical energy from a CW diode laser (669-nm output, Intense Ltd.) or a 10-Hz Nd:YAG Q-switched laser (355-nm output, New Wave Research, Inc.) was delivered into a multimode FT-400-EMT optical fiber with an SMA 905 connector (Thorlabs, Inc.). A photomultiplier tube (H10330A-45, Hamamatsu Corp.) was used to measured the $^1O_2$ luminescence intensity through a 1270-nm bandpass filter; 1270 nm is the key $^1O_2$ monomol luminescence region. Data points were registered on a 600-MHz oscilloscope, from which the $^1O_2$ decay lifetime was determined using a nonlinear least-squares curve-fitting procedure.

A polyethylene membrane with 0.05-μm pores was used which produced smaller 90-μL bubbles, compared to membranes with larger pores. At equal flow rates, smaller bubbles create larger gas−liquid interfacial areas and were shown to provide better penetration of $^1O_2$ into the bulk than the 140- and 460-μL bubbles tested previously.[7] The membranes become fragile with repeated experiments and the developing elasticity contributed some variability in the "slow" regime where slopes of plots were small or flat. Cavitation or collapse of the $^1O_2$ bubbles was not observed. Bubble speeds were determined by photography (at a shutter speed of 1/80) using a Nikon digital camera. The bubbles formed at the exterior device membrane and sometimes increased in size before dislodging from the membrane, where the emerging bubbles provided some agitation to the solution. Based on our previous work with a $^1O_2$ anthracene acceptor, we estimate that the singlet/triplet oxygen ratio in the bubble is 2.1 ppm.[7] The concentration of O_2 in water was measured with a pO_2 Sens-Ion6 oxygen electrode (Hach Co., Loveland, CO), where calibrations were done in air-saturated water. Zeroing the oxygen probe was done in oxygen-free (anoxic) solution to avoid a standard error of 0.02−0.05 mg/L. The O_2 flow rate of 60 mL/min was determined using a mass flow controller (GFC-17, Aalborg, Orangeburg, NY) connected to oxygen gas tank through a regulator.

Microbial Studies. Wild-type *E. coli* (Type CW3747) was purchased from the American Type Cells Collection (ATCC) and *Asp. fumigatus* was purchased from Fisher Scientific. *E. coli* were grown according to a previously described procedure.[13] Described here briefly, *E. coli* was revived in Luria Broth and stored at −80 °C. Quantities of *E. coli* used were in the range of 300−3000 CFU/mL and 3−30 μg/mL. *E. coli* samples were washed with 33 mM Tris-HCl buffer and the suspension was centrifuged for 20 min at 5000 rpm. Solid *E. coli* was weighed and diluted in 33 mM Tris-HCl buffer to concentrations of 3, 15, and 30 μg/mL. These samples were then purged (using either nitrogen or oxygen) for 20 min through a Pasteur pipet. The samples were oxidized with the $^1O_2$ bubbler for either 10 min (or 20 min, or 30 min, etc., up to 120 min) and 3 mL of the solution was poured onto agar plates. The samples were incubated at 37 °C for 24 h to determine the quantity of active colonies. Colony forming units (CFU) were calculated with the formula CFU = $C/(N1 + 0.1\ N2)da$, where C is the number of all counted colonies, $N1$ is the number of plates for lower bacteria dilution, $N2$ is the number of plates for higher bacteria dilution, d is the dilution factor, and a is the volume of bacteria deposited on the plate. In vitro susceptibility of *Asp. fumigatus* to 2 h of the $^1O_2$ bubble treatment was conducted with 10 and 30 μg/mL concentrations. *Asp. fumigatus* inactivation was deduced with the water suspension and cultured on agar gel. After incubation (72 h/37 °C) the colony growth was counted. The percent of *E. coli* and *Asp. fugimatus* deactivated was obtained by subtraction of colony number after treatment with and without the device from number of colony before treatment and multiplied by 100%. During the $^1O_2$ bubble treatment, the temperature of the 3-mL solution (but not the 10- or 30-mL solutions) increased by ∼5 °C in 2 h. The

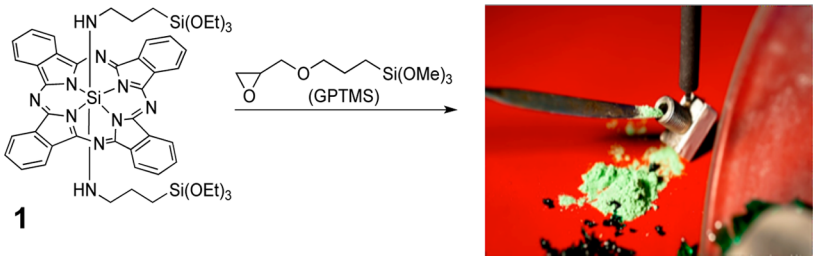

Figure 2. *Bis*-amino Si phthalocyanine **1** derivative was formed initially. Its reaction with GPTMS resulted in a Si phthalocyanine sol−gel glass that was ground and sieved to 150-μm particles, of which 35 mg was loaded into the device.

Table 1. Singlet Oxygen Bubbles Causing the Inactivation of *Escherichia coli* and *Aspergillus fumigatus*[a]

	E. coli inactivation				*Asp. fumigatus* inactivation			
pre-equilibrium condition	*E. coli* (μg/mL)	volume (mL)	% killed after 120 min	number of cells killed per bubble	*Asp. fumigatus* (μg/mL)	volume (mL)	% killed after 120 min	number of cells killed per bubble
nitrogen-presaturation[b]	30	3	90 ± 5	114	30	3	88 ± 5	111
	15	10	69 ± 4	87	10	3	70 ± 2	88
	3	30	60 ± 2	76				
air-presaturation	30	3	63 ± 5	80	30	3	62 ± 5	78
	15	10	57 ± 4	72	10	3	50 ± 4	63
	3	30	50 ± 4	63				
oxygen-presaturation[c]	30	3	8 ± 3	10	30	3	3 ± 1	4
	15	10	5 ± 1	6	10	3	2 ± 0.5	2
	3	30	3 ± 1	4				

[a]Laser light (669 nm) and O_2 gas (60 mL/min) were directed into the device. Bubbles (90 μL) emerged from the device into aqueous solution. Bubble sizes were measured from photographic images with pixel size correlations, as well as a ruler as a reference point. [b]Samples received the $^1O_2$ bubbles from the device after first being deaerated by purging with N_2 (oxygen concentration = 0.012 mM; 0.4 ppm). [c]Samples received the $^1O_2$ bubbles from the device after first being aerated by purging with O_2 (oxygen concentration = 0.83 mM; 26.6 ppm).

temperature increase in the 3-mL solution did not inactivate the bacteria or fungi, but the singlet oxygen lifetime will be slightly reduced (by ~tens of nanoseconds).[14]

For certain experiments a surfactant sodium dodecyl sulfate (SDS, Fisher Scientific, Molecular Biology grade, purity ≥99%) was added at a concentration of 8 mM, which is lower than the critical micelle concentration in water. In other experiments Ca^{2+} ions were added in the form of $CaCl_2$ (Sigma Aldrich, Bioreagent, purity ≥96%) at a concentration of 1 mM.

RESULTS AND DISCUSSION

Table 1 shows the number of *E. coli* and *Asp. fumigatus* cells killed per bubble after 120 min of exposure. The three values shown are for the three volumes tested (3, 10, and 30 mL). Since the concentration of *E. coli* decreases as the volume increases, a trend was seen where the number of cells killed per bubble also decreased as the sample volume increased. In the absence of sensitizer particles, the device (sparging O_2 with 669-nm irradiation through the membrane) showed negligible dark toxicity (<1%) to *E. coli* and *Asp. fumigatus*. Thus, the microbe inactivation is not due to mechanical stress on the cells from triplet oxygen bubbles or the red laser light of which a small amount escapes from the device into solution (approximately 0.098 mW, or 0.03% of the 383 mW laser light entering the top portion of the device is transmitted through the membrane).

Effect of Solution Presaturation. Figure 3A (solid triangles, solid circles) shows the inactivation of *E. coli* by the $^1O_2$ bubble treatment in N_2-presaturated and air-presaturated buffer solutions, respectively. The number of cells killed per bubble was 8−11 times greater in N_2- or air-pretreated water than in O_2-pretreated water (solid squares). Lower dissolved O_2 gas levels in the water sample lead to significant increases in *E. coli* killing rate.

In Figure 3A, we see a change from rapid to slow rates for bacteria inactivation occurring at approximately 50 and 60 min for the air- and nitrogen-purged samples, respectively. At this time, the oxygen concentration in solution approaches saturation as discussed below. The change from fast to slow stages in an anthracene endoperoxidation reaction was also seen, after a similar time, in our previous work.[7]

The time required to reach oxygen saturation was measured with the laser *off* and the device sparging 90-μL bubbles into 3 mL of H_2O with a gas pressure of 1 atm and an O_2 flow rate of

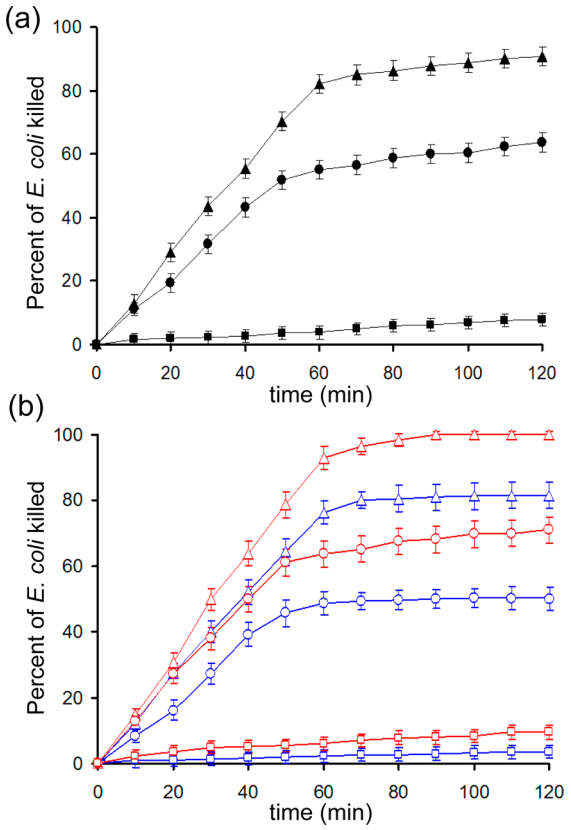

Figure 3. Experimental relationship of *E. coli* inactivation by the singlet oxygen bubble treatment: (a) in buffer solution (30 μg/mL *E. coli* in 33 mM Tris-HCl buffer) as a function of pre-equilibration with nitrogen (▲), air (●), or oxygen (■); and (b) blue symbols, SDS buffer (30 μg/mL *E. coli* in Tris-HCl buffer with sodium dodecyl sulfate (1.0 mM)), and red symbols, $CaCl_2$ buffer (30 μg/mL *E. coli* in Tris-HCl buffer with 1 mM Ca^{2+} added), after first being pre-equilibrated with nitrogen (red △, blue △), air (red ○, blue ○), or oxygen (red □, blue □). Error bars were obtained from 3 or more measurements.

60 mL/min. In water *presaturated* with air, the amount of time required to reach the oxygen saturation point was 50 ± 3 min, whereas an additional 10 min (60 ± 3 min) was required for water *presaturated* with nitrogen. The oxygen saturation levels were approached asymptotically, although an abrupt rate

dx.doi.org/10.1021/es303645n | *Environ. Sci. Technol.* 2012, 46, 12098−12104

change was observed due to the small solution volumes and relatively high oxygen flow rate (60 mL/min). Because air contains 21% oxygen, it was expected to take less time to equilibrate the O_2 concentration in a sample presaturated with air than the nitrogen-purged system.

In air-presaturated and N_2-presaturated solutions, singlet oxygen inactivated *E. coli* in two stages. The early stage was rapid and the later stage was slow, correlating to before and after O_2 saturation had been reached. In oxygen-presaturated solutions (Figure 3A, solid squares) significantly lower *E. coli* inactivation rates were observed than for nitrogen- and air-presaturated systems. There was no "rapid" phase as the solution was saturated with oxygen at $t = 0$. The *E. coli* inactivation rate, which was constant throughout this experiment is similar to the "slow" rates in the air- and nitrogen-sparged systems as shown in Table 2. Similar slopes are seen in Figure 3A for the slow phases of the nitrogen- and air-presaturated solutions, however the rate in an oxygen-purged system is only half the "slow" rate in a nitrogen-purged system (Table 2). The percent *E. coli* inactivation is shown in Figure 3 to help identify slope changes, although future research should evaluate relative germicidal effectiveness with a log scale,[15] and the time required to reach safe levels.

Table 2. Slopes of Lines from the Singlet Oxygen Bubble Treatment for Percent *E. coli* Inactivation in Figure 3

condition	rapid stage	slow stage
N_2-pre-equlibrated (open red triangles, *E. coli* + $CaCl_2$)[a]	1.57 ± 0.02	0.16 ± 0.02
N_2-pre-equlibrated (solid black triangles, *E. coli* in buffer)	1.38 ± 0.04	0.14 ± 0.03
N_2-pre-equlibrated (open blue triangles, *E. coli* + SDS)	1.28 ± 0.01	0.068 ± 0.005
air-pre-equlibrated (open red circles, *E. coli*+ $CaCl_2$)	1.22 ± 0.03	0.130 ± 0.004
air-pre-equlibrated (solid black circles, *E. coli* in buffer)	1.050 ± 0.003	0.12 ± 0.01
air-pre-equlibrated (open blue circles, *E. coli* + SDS)	0.95 ± 0.03	0.050 ± 0.007
O_2-pre-equlibrated (open red squares, *E. coli*+ $CaCl_2$)	0.07 ± 0.03	
O_2-pre-equlibrated (solid black squares, *E. coli* in buffer)	0.06 ± 0.02	
O_2-pre-equlibrated (open blue squares, *E. coli* + SDS)	0.028 ± 0.006	

[a]The last 3 data points were ignored since 100% inactivation had been reached.

Effect of SDS Addition. The literature indicates that bacteria preferentially accumulate at the water−air interface,[16] as the energy is reduced when the hydrophobic portions of the cells are in contact with air. Bacteria with greater hydrophobic character are more strongly attracted to this interface.[17] A surfactant such as sodium dodecyl sulfate (SDS) efficiently removes bacteria adhered to surfaces[18] and increases the negative charge at the interface.[19] Since surfactants are also strongly attracted to the air−water interface our hypothesis was that SDS would preferentially occupy the air−water interface of the bubbles by displacing the bacteria, effectively decreasing the bacteria concentration within the diffusion length of singlet oxygen (~150 nm). This would result in a decrease of the kill rates compared to rates with no SDS.

In air-presaturated and N_2-presaturated solutions, addition of SDS (1 mM) led to reduced efficiency in *E. coli* inactivation, that is, a 12% reduction for N_2 and 9% reduction for air after 120 min of exposure (Figure 3B, blue symbols). Not only is the overall percentage of killed *E. coli* organisms reduced by the addition of SDS, but the rate of killing is more significantly reduced during the "slow" phase (i.e., after the solution becomes saturated with O_2). Whereas the rate is reduced by 8% during the rapid phase in a N_2-presatured solution, the rate is reduced by 50% during the slow phase (Table 2). Similarly, in an air-presaturated solution, the fast rate is reduced by ~10% whereas the slow rate is reduced by 60% in the presence of SDS.

Effect of Ca^{2+} Addition. A separate set of experiments were conducted to determine the effect of higher ionic strength of the solution on the inactivation of *E. coli* by $^1O_2$. Higher ionic strength, achieved by the addition of Ca^{2+} ions, reduces the zeta potential on the bacteria surface and so tends to increase bacteria accumulation at the air−water interface.[16] As the *E. coli* surface has negative charges which can be partially neutralized with added Ca^{2+} ions, *E. coli* self-repulsion may be decreased.[19] Indeed, addition of Ca^{2+} ions to the solution resulted in a significant increase in the rate of bacteria kill rates compared to the standard buffered solution. *E. coli* kill rates, during the rapid phase, were observed to increase by 14% and 16% when $CaCl_2$ (1 mM) was added to nitrogen or air presaturated solutions, respectively. The kill rate reached 100% in less than 90 min for the nitrogen-sparged solution containing calcium ions. In the "slow" phase, the magnitude of the effect of Ca^{2+} addition is comparable as the slopes increased by 18% and 5% in nitrogen and air presaturated solutions, respectively. In oxygen, no significant effect of Ca^{2+} addition could be discerned as the small slope increase was within measurement error. These observations stand in stark contrast to the results from SDS addition, where kill rates of bacteria decreased upon addition of the surfactant.

Fungi Inactivation. The bacteria and fungi exhibited similar inactivation rates (Table 1). Figure 4 shows the results of *Asp. fumigatus* inactivation after 120 min of exposure to the $^1O_2$ bubbler. Here also, the maximum rate for $^1O_2$ bubble toxicity to inactivate *Asp. fumigatus* was in a N_2 presaturated solution. In a solution presaturated with air, the percent of fungi killed was approximately 30% lower than that for the N_2 presaturated solution. Similar to the *E. coli* data, a substantially lower percent of the fungi are killed in a solution presaturated with O_2 (5% vs 90% in nitrogen).

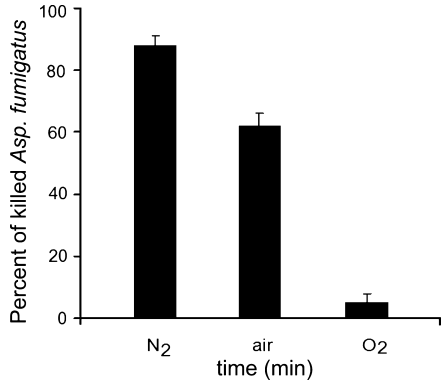

Figure 4. Singlet oxygen bubble treatment leading to *Asp. fumigatus* inactivation (10 μg/mL *Asp. fumigatus* in 33 mM Tris-HCl buffer) in solutions after first being pre-equilibrated with nitrogen, air, or oxygen.

Time Scales. Our results show that the bubble lifetime was longer than the singlet oxygen lifetime (τ_Δ) in solution (Table 3). The bubbles traversed a 5 mm distance in 1/80 s and so

Table 3. Lifetime of Singlet Oxygen (τ_Δ) in Air or Delivered via Gas Bubbles into H_2O and D_2O, in the Presence and Absence of Sodium Azide[a]

	medium	τ_Δ (μs)	τ_Δ (μs) with $^1O_2$ quenching by NaN_3[b]	comments
1	gas stream from device	1050 ± 15	NA	$^1O_2$ stream into air[c]
2	core of gas bubble	980 ± 20	no effect	$^1O_2$ encapsulated in gas bubble
3	H_2O	4.5 ± 0.2	0.2 ± 0.1	$^1O_2$ solvated
4	D_2O	66.0 ± 0.3	3.40 ± 0.03	

[a]Partially aerated H_2O with 10−20 min O_2 flushing from device, $[O_2]$ = 5−15 ppm. [b]$[NaN_3]$ = 10 μM. [c]Flowing gas stream (solvent free).

travel at a velocity of approximately 400 mm/s, which is similar to velocities measured by Leifer et al. of slightly larger-sized bubbles using Stokes Law.[20] The total distance the bubble travels was 7 mm, which took 17.7 ± 0.5 ms. Figure 5 suggests

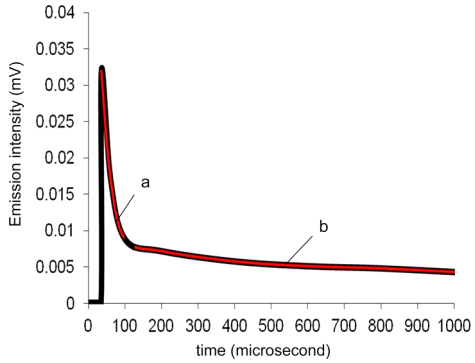

Figure 5. Singlet oxygen decay curves in air-presaturated H_2O: (a) fast decay component attributed to solvated singlet oxygen, and (b) slow decay component attributed to singlet oxygen within the interior of the gas bubble. Experimental data (black line) and fitting (red line) are shown.

a decreased τ_Δ on going from the gas bubble (0.98 ± 0.02 ms) to H_2O (4.5 ± 0.2 μs), from two decay components observed in the 1270 nm phosphorescence upon irradiation of the sensitizer particles with 355 nm. Singlet oxygen lifetime in the interior of the bubble was longer due to reduced encounters with water molecules than after diffusion into the bulk. In air, a singlet oxygen lifetime of 86 ms has been previously calculated,[21] which will be sensitive to factors such as humidity and solid-surface physical quenching. In previous work, Scaiano et al. found short and long singlet oxygen lifetimes depending whether it resided within porous zeolite structures or in the bulk media.[22] Our results are in-line with the literature lifetime value of $^1O_2$ solvated in H_2O (3.5 μs).[14,23] That the oxygen bubbling device leads to solvated $^1O_2$ seems probable since (i) the τ_Δ increased in D_2O solvent (found 66.0 ± 0.3 μs; lit. data[14] of τ_Δ = 65 μs in homogeneous D_2O) compared to H_2O, (ii) the emission intensity of the fast decay component of singlet oxygen in Figure 5 decreased by 4-fold to 0.008 ± 0.002 mV in O_2 presaturated solution (high dissolved O_2 resulting in low $^1O_2$ mass transfer into the solution), and (iii) the τ_Δ decreased when NaN_3, an effective singlet oxygen quencher, was added, e.g. 10 μM NaN_3 in H_2O (found 0.2 ± 0.1 μs; lit. data[24] of τ_Δ = 0.18 μs in homogeneous H_2O with 10 μM NaN_3). The distance that solvated singlet oxygen travels in H_2O is reported to be ∼150 nm and ∼20 times higher in D_2O, and in air the distance is reported to be ∼1.0−1.5 mm.[25−27] The $^1O_2$ bubbles traversed a distance of 0.39 mm in water in 0.98 ms (lifetime of singlet oxygen in bubble). Once the bubble was carried 7 mm to the air−water interface and burst, it contained only $^3O_2$. Collisions between bubbles[28] at the outer air−water interface were not studied since they contained no $^1O_2$.

Mechanism. We posit two mechanisms: (1) dissolution and (2) gas bubble−liquid interface.

(1) Dissolution where singlet oxygen solvation into and diffusion through the water takes place and accounts for the "fast" rate of killing organisms in nitrogen and air purged solutions. Fick's Law appears to dominate since $^1O_2$ transport from the bubble to solution was enhanced by reduced dissolved oxygen concentrations in the solutions. Oxygen flux from an oxygen bubble to a nitrogen-, air-, or oxygen-saturated water can be calculated by using the Stagnant Boundary Layer Model[29] in which flux is proportional to the concentration gradient:

$$F = -D\frac{\delta[A]}{\delta[Z]} \quad \text{(eq 1)}$$

where D is the molecular diffusion coefficient, $\delta[Z]$ is the thickness of the stagnant film, and $\delta[A]$ is the concentration difference across the film. Because of the limited lifetime of singlet oxygen in the gas phase, singlet oxygen is available only during the first 0.98 ms or 0.39 mm of the bubble's travel from the device membrane to the surface. The outer layer of the bubble may be a hotspot for $^1O_2$, but penetration into H_2O produces an even shorter $^1O_2$ lifetime of 4.5 μs. Once solvated in H_2O, the distance that $^1O_2$ travels is less than 200 nm.[30] Once the solution becomes saturated with oxygen, further diffusion of singlet oxygen from newly generate bubbles is suppressed.

(2) A gas bubble−liquid interface reaction via direct collision of singlet oxygen with the microbe may occur at all stages of the reaction and accounts for the reduced rate of killing organisms in the "slow" phase of the reaction (i.e., after the solution becomes saturated with O_2). Here, singlet oxygen in the gas phase collides with the liquid interface and reacts with microbes present (or near) the interface with essentially no diffusion. The mechanism is relatively independent of dissolved oxygen concentration and occurs at a much slower rate than the dissolution mechanism. The results imply that $^1O_2$, even when not fully solvated, can inactivate microbes. This is due to the tendency of *E. coli* to accumulate at the gas−liquid interface defining the bubble. By modifying the tendency of bacteria to accumulate at the bubble interface, significant differences in the rate of bacterial inactivation by direct impingement of singlet oxygen were demonstrated. Increased effectiveness of inactivating *E. coli* was achieved by the addition of $CaCl_2$. This dication reduced the surface charge of the bacteria, thereby reducing its hydrophilicity and reducing its tendency to self-repel. As a result, *E. coli* could more effectively accumulate at the interface and so be more susceptible to collisions with singlet oxygen. In contrast, addition of SDS served to displace *E. coli* at the interface, thereby reducing bacterial accumulation on the bubble interface and reducing the probability of contact with singlet oxygen on the gas−liquid interface.

Previous studies have shown that bacteria,[16,17] as well as particles,[19] accumulate at the air−water interface due to wetting properties and surface charges of the particulate surfaces. Bacteria with hydrophobic wetting properties and low zeta potentials are especially strongly attracted to the gas−liquid interface, minimizing the overall energy of the system. A singlet oxygen bubble reactor can take advantage of this bacterial accumulation to increase overall toxicity.

Technical Implications. The disinfection method described here produces bubbles enriched in $^1O_2$ and leaves behind no waste products other than $^3O_2$ in solution. The photocatalyst is physically separated from the liquid and so cannot inadvertently contaminate the solution. For any one bubble a finite amount of singlet oxygen diffuses into water. Singlet oxygen concentration is significant only during the first 0.98 ms of the bubble lifetime in water (in this study, the total bubble lifetime was 17.7 ms). Thus only the first millisecond needs to be considered since $^1O_2$ has decayed to an insignificant concentration after that time. The relatively short lifetime of singlet oxygen makes this device different from conventional bubble reactors, which typically consider O_2 diffusion over the whole path of the bubble as well as the concentration gradient in the liquid.[8]

Low dissolved O_2 gas concentrations assist $^1O_2$ mass transfer to the bulk solution. The bubbles containing $^1O_2$ were shown to inactivate *E. coli* and *Asp. fumigatus* more efficiently in nitrogen-deaerated solutions than solutions presaturated with air. That the device delivers $^1O_2$ more efficiently in nitrogen-deaerated solutions is unconventional as common photosensitized $^1O_2$ disinfection methods require aerobic solutions. Oxygen presaturation minimizes $^1O_2$ diffusion into solution and essentially eliminates this relatively rapid mechanism for destroying *E. coli* and *Asp. fumigatus*.

A second mechanism was also identified where $^1O_2$ interacts with *E. coli* at or near the gas−liquid interface. This mechanism operates at a rate that is approximately 10 times slower than the dissolution and diffusion mechanism discussed above.

The rate of the $^1O_2$ mechanisms can be increased by increasing the tendency of *E. coli* to accumulate at the bubble surface (e.g., addition of Ca^{2+}) or can be decreased by addition of a surfactant that preferentially accumulates at the bubble surface. Since $^1O_2$ can only travel ∼150 nm in solution before decaying to $^3O_2$, increased concentration of bacteria near the bubble surface serves to increase the effectiveness of both mechanisms and thus the overall toxicity of $^1O_2$ bubbles.

The challenge in developing the device further is to provide a low cost way to suit disinfection needs. This will include specialized interchangeable components, such as LEDs or sunlight collimators to replace the diode laser used in this experiment. Costs could be further reduced by using photosensitizers from plant products or readily available starting materials with wavelength-selective absorptivities.

AUTHOR INFORMATION

Corresponding Author

*E-mail: agreer@brooklyn.cuny.edu.

Notes

The authors declare no competing financial interest.

ACKNOWLEDGMENTS

D.B., D.A., and A.G. acknowledge support from the National Institute of General Medical Sciences (NIH SC1GM093830). A.M.L. acknowledges support from the NYS Empire State Development's Division of Science, Technology & Innovation (NYSTAR). We thank Milt Rosen for insightful discussions. We thank Alison Domzalski for the photography work and Leda Lee for the graphic arts work.

REFERENCES

(1) Manjón, F.; Villén, L.; García-Fresnadillo, D.; Orellana, G. On the factors influencing the performance of solar reactors for water disinfection with photosensitized singlet oxygen. *Environ. Sci. Technol.* **2008**, *42*, 301−307.

(2) Cho, M.; Lee, J.; Mackeyev, Y.; Wilson, L. J.; Alvarez, P. J. J.; Hughes, J. B.; Kim, J.-H. Visible light sensitized inactivation of MS-2 bacteriophage by a cationic amine-functionalized C_{60} derivative. *Environ. Sci. Technol.* **2010**, *44*, 6685−6691.

(3) Chen, Y.; Lu, A.; Li, Y.; Zhang, L.; Yip, H. Y.; Zhao, H.; An, T.; Wong, P.-K. Naturally occurring sphalerite as a novel cost-effective photocatalyst for bacterial disinfection under visible light. *Environ. Sci. Technol.* **2011**, *45*, 5689−5695.

(4) Wang, W.; Yu, Y.; An, T.; Li, G.; Yip, H. Y.; Yu, J. C.; Wong, P. K. Visible-light-driven photocatalytic inactivation of *E. coli* K-12 by bismuth vanadate nanotubes: Bactericidal performance and mechanism. *Environ. Sci. Technol.* **2012**, *46*, 4599−4606.

(5) Chen, C. C.; Ma, W. H.; Zhao, J. C. Semiconductor-mediated photodegradation of pollutants under visible-light irradiation. *Chem. Soc. Rev.* **2010**, *39*, 4206−4219.

(6) Marin, M. L.; Santos-Juanes, L.; Arques, A.; Amat, A. M.; Miranda, M. Organic photocatalysts for the oxidation of pollutants and model compounds organic photocatalysts for the oxidation of pollutants and model compounds. *Chem. Rev.* **2012**, *112*, 1710−1750.

(7) Bartusik, D.; Aebisher, D.; Ghafari, B.; Lyons, A. M.; Greer, A. Generating singlet oxygen bubbles: A new mechanism for gas-liquid oxidations in water. *Langmuir* **2012**, *28*, 3053−3060.

(8) Davidovits, P.; Kolb, C. E.; Williams, L. R.; Jayne, J. T.; Worsnop, D. R. Mass accommodation and chemical reactions at gas-liquid interfaces. *Chem. Rev.* **2006**, *106*, 1323−1354.

(9) Villén, L.; Francisco, M.; García-Fresnadillo, D.; Orellana, G. Solar water disinfection by photocatalytic singlet oxygen production in heterogeneous medium. *Appl. Catal. B: Environ.* **2006**, *69*, 1−9.

(10) Chemburu, S.; Corbitt, T. S.; Ista, L. K.; Ji, E.; Fulghum, J.; Lopez, G. P.; Ogawa, K.; Schanze, K. S.; Whitten, D. G. Light-induced biocidal action of conjugated polyelectrolytes supported on colloids. *Langmuir* **2008**, *24*, 11053−11062.

(11) Funes, M. D.; Caminos, D. A.; Alvarez, M. G.; Fungo, F.; Otero, L. A.; Durantini, E. N. Photodynamic properties and photoantimicrobial action of electrochemically generated porphyrin polymeric films. *Environ. Sci. Technol.* **2009**, *43*, 902−908.

(12) Benabbou, A. K.; Guillard, C.; Pigeot-Rémy, S.; Cantau, C.; Pigot, T.; Lejeune, P.; Derriche, Z.; Lacombe, S. Water disinfection using photosensitizers supported on silica. *J. Photochem. Photobiol. A: Chem.* **2011**, *219*, 101−108.

(13) Aebisher, D.; Zamadar, M.; Mahendran, A.; Ghosh, G.; McEntee, C.; Greer, A. Fiber-optic singlet oxygen [$^1O_2$ ($^1\Delta_g$)] generator device serving as a point selective sterilizer. *Photochem. Photobiol.* **2010**, *86*, 890−894.

(14) Jensen, R. L.; Arnbjerg, J.; Ogilby, P. R. Temperature effects on the solvent-dependent deactivation of singlet oxygen. *J. Am. Chem. Soc.* **2010**, *132*, 8098−8105.

(15) *The Science of Photobiology*; Smith, K. C., Ed.; Plenum Publishing Corp.: New York, 1977; pp 407−410.

(16) Schäfer, A.; Harms, H.; Zehnder, A. J. B. Bacterial accumulation at the air-water interface. *Environ. Sci. Technol.* **1998**, *32*, 3704−3712.

(17) Henk, M. C. Method for collecting air-water interface microbes suitable for subsequent microscopy and molecular analysis in both research and teaching laboratories. *Appl. Environ. Microbiol.* **2004**, *70*, 2486−2493.

(18) Drumm, B.; Neumann, A. W.; Policova, Z.; Sherman, P. M. Bacterial cell surface hydrophobicity properties in the mediation of in

vitro adhesion by the rabbit enteric pathogen *Escherichia coli* strain RDEC-1. *J. Clin. Invest.* **1989**, *84*, 1588−1594.
(19) Rosen, M. J. *Surfactants and Interfacial Phenomena*; 2nd ed.; Wiley: New York, 1989; pp 36−38, 384, and 385.
(20) Leifer, I.; Patro, R.; Bowyer, P. J. A study on the temperature variation of rise velocity for large clean bubbles. *Atmos. Oceanic Technol.* **2000**, *17*, 1392−1402.
(21) Schweitzer, C.; Schmidt, R. Physical Mechanisms of Generation and Deactivation of Singlet Oxygen. *Chem. Rev.* **2003**, *103*, 1685−1757.
(22) Cojocaru, B.; Laferrière, M.; Carbonell, E.; Parvulescu, V.; García, H.; Scaiano, J. C. Direct time-resolved detection of singlet oxygen in zeolite-based photocatalysts. *Langmuir* **2008**, *24*, 4478−4481.
(23) Maisch, T.; Baier, J.; Franz, B.; Maier, M.; Landthaler, M.; Szeimies, R.-M.; Bäumler, W. The role of singlet oxygen and oxygen concentration in photodynamic inactivation of bacteria. *Proc. Natl. Acad. Sci., U.S.A.* **2007**, *104*, 7223−7228.
(24) Wessels, J. M.; Rodgers, M. A. J. Detection of the $O_2(^1\Delta_g)$-$O_2(^3\Sigma_g^{-1})$ transition in Aqueous Environments: A Fourier-transform near-infrared luminescence study. *J. Phys. Chem.* **1995**, *99*, 15725−15727.
(25) Midden, W. R.; Wang, S. Y. Singlet oxygen generation for solution kinetics: Clean and simple. *J. Am. Chem. Soc.* **1983**, *105*, 4129−45.
(26) Dahl, T. A.; Midden, W. R.; Hartman, P. E. Pure singlet oxygen cytotoxicity for bacteria. *Photochem. Photobiol.* **1987**, *46*, 345−352.
(27) Naito, K.; Tachikawa, T.; Cui, S.-U.; Sugimoto, A.; Fujitsuka, M.; Majima, T. Single-molecule detection of airborne singlet oxygen. *J. Am. Chem. Soc.* **2006**, *128*, 16430−16431.
(28) Zawala, J.; Malysa, K. Influence of the impact velocity and size of the film formed on bubble coalescence time at water surface. *Langmuir* **2011**, *27*, 2250−2257.
(29) Liss, P. S.; Slater, P. G. Flux of gases across the air-sea interface. *Nature* **1974**, *247*, 181−184.
(30) Skovsen, E.; Snyder, J. W.; Lambert, J. D. C.; Ogilby, P. R. Lifetime and diffusion of singlet oxygen in a cell. *J. Phys. Chem. B* **2005**, *109*, 8570−8573.